Journal of Hydraulic Research Vol. 47, No. 1 (2009), pp. 29–40
doi:10.3826/jhr.2009.2954

Turbulence measurements in positive surges and bores

Mesures de turbulence dans les intumescences et les ressauts

CHRISTIAN KOCH, *Division of Civil Engineering, The University of Queensland, Brisbane QLD 4072, Australia*

HUBERT CHANSON, (IAHR Member), *Professor in Civil Engineering, The University of Queensland, Brisbane QLD 4072, Australia. Fax: (61 7) 33 65 45 99; e-mail: h.chanson@uq.edu.au; http://www.uq.edu.au/~e2hchans/*

ABSTRACT
A positive surge results from a sudden change in flow that increases the flow depth. New experiments were conducted in a large channel. Most positive surge tests were conducted with a horizontal bed slope, a constant flow rate and uncontrolled flow conditions. The only dependant variable was the downstream gate opening after closure. Detailed turbulence measurements were performed with high-temporal resolution using side-looking acoustic Doppler velocimetry. Two types of positive surge were observed: undular surge for Froude numbers less than 1.7, and weak (breaking) surges above. Instantaneous velocity measurements beneath advancing surges showed a marked effect of the surge passage on the velocity field. Streamwise velocities showed rapid flow deceleration at all vertical elevations. Large fluctuations of longitudinal and transverse velocities were recorded beneath the surges, including some unsteady flow recirculation beneath a weak surge front. Turbulent stresses were deduced from high-pass filtered data. The results showed large normal and tangential Reynolds stresses beneath the surges. A comparison between undular and weak surges suggested some major difference. In weak surge flows, the data showed rapid flow separation beneath the surge front. In undular surges, maximum Reynolds stresses were observed beneath and just before each wave crest behind the leading wave.

RÉSUMÉ
Une onde positive résulte d'un changement soudain de l'écoulement qui augmente le tirant d'eau. De nouvelles expériences ont été entreprises dans un grand canal. La plupart des essais de montée subite ont été effectués avec une pente horizontale de lit, un débit constant et des états non contrôlés d'écoulement. La seule variable indépendante était l'ouverture d'une vanne aval initialement fermée. Des mesures instantanées de turbulence ont été effectuées avec une haute résolution temporelle en utilisant un vélocimètre acoustique Doppler. On a observé deux types d'onde positive: intumescence ondulée pour un nombre de Froude inférieur à 1.7, et un faible ressaut (déferlant) au-delà. Les mesures instantanées de vitesse sous les ondes en progression ont montré un effet marqué de la montée subite sur le champ de vitesse. Les vitesses longitudinales ont montré une décélération rapide sur toute la profondeur. De grandes fluctuations des vitesses longitudinales et transversales ont été enregistrées sous les ondes, y compris des recirculations instables d'écoulement sous un front d'onde de faible ressaut. Des efforts turbulents ont été déduits des données filtrées passe-haut. Les résultats ont montré de grandes contraintes de Reynolds normales et tangentielles sous les ressauts. Une comparaison entre les ressauts faibles et les intumescences ondulées a suggéré quelques différences majeures. Dans les ressauts faibles, les données ont montré une variation rapide de l'écoulement sous le front. Dans les intumescences ondulées, on a observé des contraintes de Reynolds maximum en dessous et juste devant chaque crête de vague derrière la vague principale.

Keywords: Acoustic Doppler velocimetry, bores, physical modelling, positive surge, turbulence, turbulent velocity measurements

1 Introduction

A positive surge results from a sudden change in flow that increases the depth: e.g., a partial or complete closure of a gate (e.g., Henderson, 1966; Chanson, 2004a) (Fig. 1). Positive surges are commonly observed in man-made channels. They may be induced by control structures (e.g., gates) installed along water supply canals for irrigation and water power purposes. Another form of positive surge is the tidal bore. Although a positive surge may be analysed using a quasi-steady flow analogy, its inception and development is commonly predicted using the method of characteristics and Saint-Venant equations (Barré de Saint-Venant, 1871). After formation of the surge, the flow properties immediately upstream and downstream of the front must satisfy the continuity and momentum principles (e.g., Rayleigh, 1908; Henderson, 1966; Liggett, 1994; Chanson, 2004a,b). For a "fully-developed positive" surge, the positive surge is seen by an observer travelling at the surge speed U as a quasi-steady flow situation called a "hydraulic jump in translation" (Fig. 1). In a rectangular, horizontal channel and neglecting friction loss, the

Revision received November 8, 2006/Open for discussion until August 31, 2009.

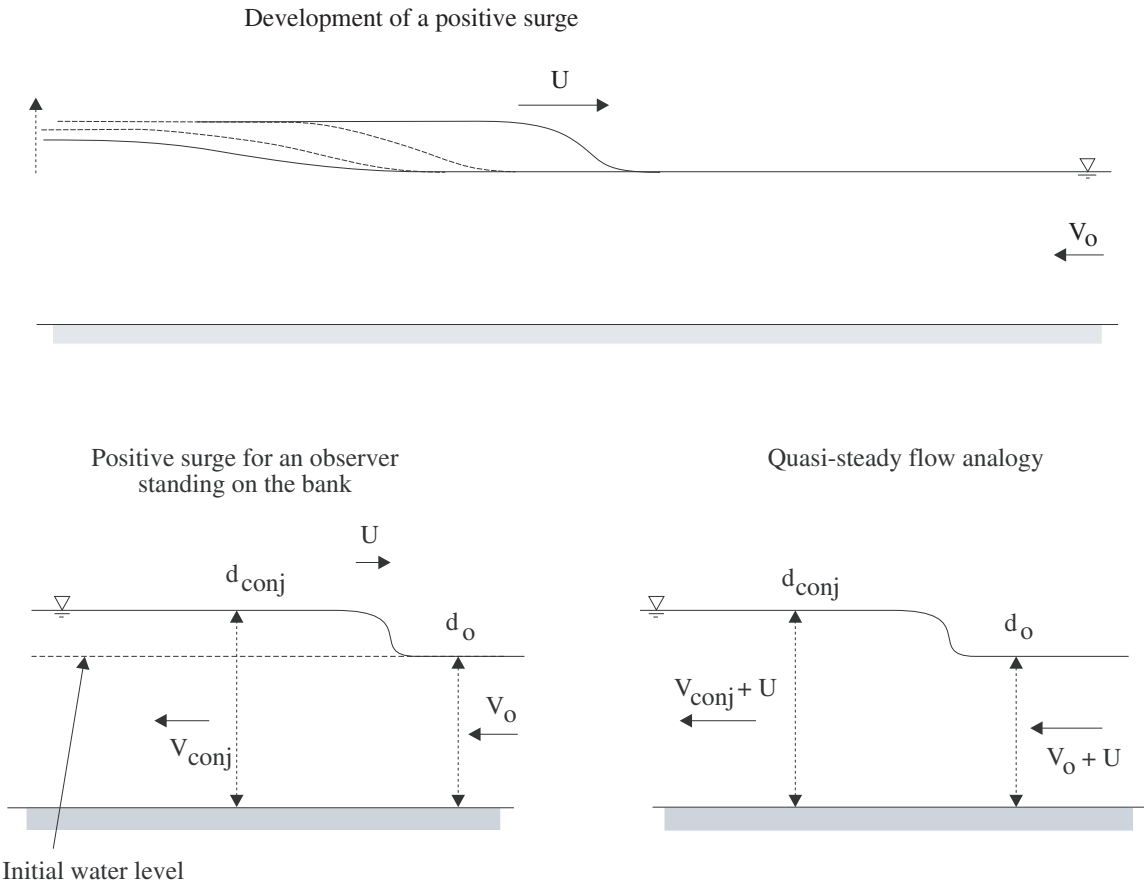

Figure 1 Definition sketch of a positive surge

solution of the continuity and momentum equations applied to a control volume across the surge front yields:

$$\frac{d_{conj}}{d_o} = \frac{1}{2} \times \left(\sqrt{1 + 8 \times Fr^2} - 1\right) \quad (1)$$

$$\frac{Fr_{conj}}{Fr} = \frac{2^{3/2}}{\left(\sqrt{1 + 8 \times Fr^2} - 1\right)^{3/2}} \quad (2)$$

where d_{conj} and d_o are respectively, the new and initial flow depths (Fig. 1), and the Froude numbers Fr and Fr_{conj} are the surge Froude numbers defined respectively as:

$$Fr = \frac{V_o + U}{\sqrt{g \times d_o}} \quad (3)$$

$$Fr_{conj} = \frac{V_{conj} + U}{\sqrt{g \times d_{conj}}} \quad (4)$$

where U is the surge velocity as seen by a stationary observer on the channel bank and positive in the upstream direction, V is the flow velocity, the subscript o refers to the initial flow conditions and the subscript conj refers to the new (conjugate) flow conditions (Fig. 1).

Positive surges were studied by hydraulicians and applied mathematicians for a few centuries. Pertinent reviews comprised Benjamin and Lighthill (1954), Sander and Hutter (1991), and Cunge (2003). Major contributions included the works of Barré de Saint-Venant (1871), Boussinesq (1877), and more recently Lemoine (1948), Serre (1953) and Benjamin and Lighthill (1954). Several researchers discussed the development of a positive surge (e.g., Tricker, 1965; Peregrine, 1966; Wilkinson and Banner, 1977; Teles Da Silva and Peregrine. 1990; Sobey and Dingemans, 1992). Classical experimental investigations of undular surges included Bazin (1865), Favre (1935), Zienkiewicz and Sandover (1957), Sandover and Holmes (1962), Benet and Cunge (1971). Ponsy and Carbonnell (1966) and Treske (1994) presented a comprehensive description of positive surges in trapezoidal channels of large sizes.

To date, most experimental studies were limited to visual observations and sometimes free-surface measurements. These rarely encompassed turbulence except in a few limited studies (e.g., Yeh and Mok, 1990; Hornung *et al.*, 1995). It is the purpose of this paper to document the flow field and turbulence characteristics in positive surges under controlled flow conditions. New free-surface and turbulent velocity measurements were performed in a large-size laboratory facility. The unsteady flow results provide an unique characterisation of the advancing bore front, of the unsteady turbulent velocity field, and of the associated turbulent mixing processes. The findings yield a new understanding of positive surge hydrodynamics.

2 Experimental facility and methods

New experiments were performed in a large tilting flume at the University of Queensland. The channel was 0.5 m wide 12 m long

and it was horizontal for most experiments. The flume was made of smooth PVC bed and glass walls, and waters were supplied by a constant head tank. A tainter gate was located next to the downstream end.

The water discharge was measured with bend meters which were calibrated *in-situ* with a large V-notch weir. The percentage of error was expected to be less than 2%. In steady flows, water depths were measured using rail mounted pointer gauges and acoustic displacement meters. Unsteady water depths are measured with acoustic displacement meters Microsonic™ Mic + 25/IU/TC with an accuracy of 0.18 mm and a response time of 50 ms. Pressure and velocity measurements in steady flows were performed with a Prandtl–Pitot tube (3.3 mm Ø) which was previously calibrated as a Preston tube based upon *in-situ* experiments (Chanson, 2000). Turbulent velocity measurements were conducted with an acoustic Doppler velocimeter Sontek™ 16 MHz micro-ADV (Acoustic Doppler Velocimetry) equipped with a two-dimensional side-looking head. For the experiments, the velocity range was 1.0 m s^{-1}, the sampling rate was 50 Hz and the data accuracy was 1%.

The translation of Pitot-Prandtl and ADV probes in the vertical direction was controlled by a fine adjustment travelling mechanism connected to a Mitutoyo™ digimatic scale unit. The error on the vertical position of the probe was $\Delta z < 0.025$ mm. The accuracy on the longitudinal position was estimated as $\Delta x > \pm$ 2 mm. The accuracy on the transverse position of the probe was less than 1 mm.

Additional information was obtained with digital cameras Panasonic™ Limux DMC-FZ20GN (shutter: 8 to 1/2000 sec) and Canon™ A85 (shutter: 15 to 1/2000 sec), and a digital videocamera Sony™ DV-CCD DCR-TRV900 (speed 25 fr/sec, shutter: 1/4 to 1/10,000 sec). Further details on the experimental facility were reported in Koch and Chanson (2005).

2.1 Acoustic Doppler velocity metrology

ADV measurements are performed by measuring the velocity of particles in a remote sampling volume based upon the Doppler shift effect (e.g., Voulgaris and Trowbridge, 1998; McLelland and Nicholas, 2000). An ADV system records simultaneously four values with each component of a sample: the velocity component, the signal strength value, the correlation value and the signal-to-noise ratio. Past and present experiences demonstrated many problems because the signal outputs combine the effects of velocity fluctuations, Doppler noise, signal aliasing, turbulent shear and other disturbances (Lemmi and Lhermitte, 1999; Goring and Nikora, 2002; Chanson *et al*., 2005). For all experiments, present experience demonstrated recurrent problems with the velocity data, including low correlations and low signal to noise ratios. The situation improved drastically by mixing some vegetable dye (Dytex Dye™ Ocean Blue) in the entire water recirculation system. Other problems were experienced with boundary proximity.

In steady flows, detailed comparisons between ADV and Prandtl–Pitot tube data were conducted at $y = 0.473$, 0.450, and 0.375 m (or 27, 50, and 125 mm from the left sidewall) with the micro ADV sensors facing the left sidewall, where y is the transverse distance from the right wall. Experimental data indicated that the streamwise velocity data were not affected by the presence of the channel bed at $y = 0.450$ and 0.375 m as observed at $y = 0.250$ m. But the ADV data underestimated the velocity in the vicinity of a sidewall ($y > 0.455$ mm). This was associated with a drastic decrease in average signal correlations, average signal-to-noise ratios and amplitudes next to the wall (Koch and Chanson, 2005).

While several ADV post-processing techniques were devised for steady flows (e.g. Goring and Nikora, 2002; Wahl, 2003), these post-processing techniques are not applicable to unsteady flows (e.g., Nikora, 2004; *Person. Comm.*, Chanson *et al*., 2005). In the present study, unsteady flow post-processing was limited to a removal of communication errors and a replacement by interpolation.

2.2 Reynolds stress estimates in rapidly-varied flow motion

In turbulence studies, the measured statistics are based upon the analysis of instantaneous turbulent velocity data: $v = V - \bar{V}$, where $\bar{V}$ is a time-average velocity. If the flow is "gradually-varied", $\bar{V}$ must be a low-pass filtered velocity component, or variable-interval time average VITA (Piquet, 1999). The cut-off frequency must be selected such that the averaging time is greater than the characteristic period of fluctuations, and small with respect to the characteristic period for the time-evolution of the mean properties (e.g. Garcia and Garcia, 2006). In highly unsteady flows, experiments have to be repeated many times, and the turbulent velocity fluctuation becomes the deviation of the instantaneous velocity from the ensemble average is (Bradshaw, 1971).

In undular surge flows, the Eulerian flow properties showed an oscillating pattern with a period of about 2.4 s that corresponded to the period of the free-surface undulations. The unsteady data were therefore filtered with a low/high-pass filter threshold greater than 0.4 Hz (i.e. 1/2.4 s) and smaller than the Nyquist frequency (herein 25 Hz). The cutoff frequency was selected as 1 Hz based upon a detailed sensitivity analysis (Koch and Chanson, 2005). The same filtering technique was applied to both streamwise and transverse velocity components, and for both weak and undular surge experiments. Reynolds stresses were calculated from the high-pass filtered signals.

2.3 Positive surge generation

The study of positive surges was conducted with one set of initial flow conditions (Table 1). The experimental setup was selected to generate both undular bores and breaking surges with the same initial conditions. The only dependant parameter was the downstream gate opening after closure. Steady gradually-varied flow conditions were established for at least 10 min prior to measurements and flow measurements data acquisition were started 2 min prior to gate closure. A positive surge was generated by the rapid

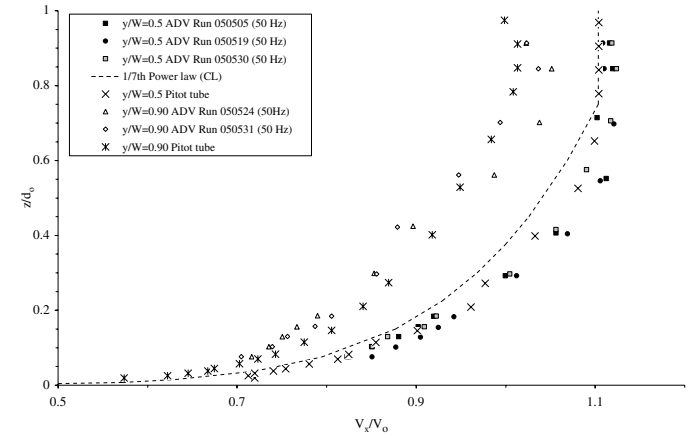

(a)

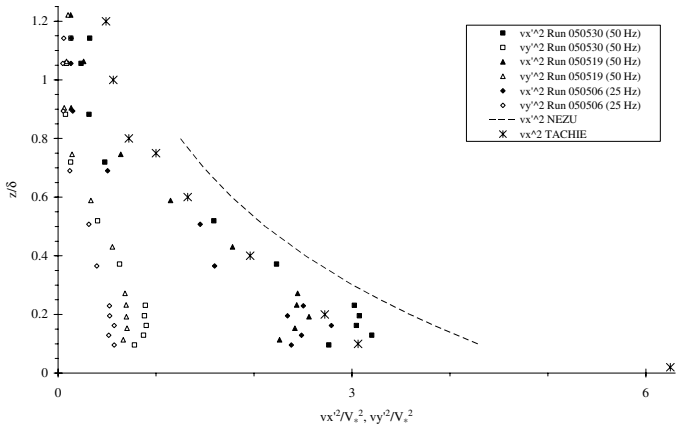

(b)

Figure 2 Dimensionless velocity distributions in the initial steady flow at $x = 5$ m for $Q = 0.040\,\mathrm{m^3\,s^{-1}}$, $d_o = 0.079$ m. (a) Time-averaged velocities V_x/V_o — Comparison between Prandtl–Pitot tube data, ADV data, and 1/7th power law. (b) Turbulent velocity distributions $v_x'^2/V^{*2}$ and $v_y'^2/V^{*2}$ on channel centreline — Comparison with Nezu's (2005) experimental correlations and data by Tachie (2001)

partial closure of the downstream gate. After closure the bore propagated upstream and each experiment was stopped when the bore front reached the intake structure. Detailed velocity measurements were performed at a distance $x = 5$ m downstream of the channel intake and at $y/W = 0.5$ (channel centreline), 0.75, 0.90 and 0.95, where W is the channel width ($W = 0.5$ m). Acoustic displacement meters were located at $x = 10.95$ m, 7.25 m, 6 m, 5.1 m and 5 m. The latter sampled the free-surface elevation immediately above the ADV sampling volume.

The initial steady flow was partially-developed with $\delta/d_o = 0.6$ to 0.8 at $x = 5$ m (Fig. 2). Figure 2(a) presents the dimensionless vertical velocity profile on the channel centreline ($y/W = 0.5$) and close to the wall ($y/W = 0.9$). Both ADV and Prandtl–Pitot tube data are reported and they are compared with a 1/7th power law. The shear velocity was estimated using both Preston–Prandtl–Pitot tube and a match between velocity data in the inner flow layer and logarithmic velocity law. The results were close and they yielded: $V^* = 0.044$ m/s. Figure 2(b) presents dimensionless distributions of normal Reynolds stresses $v_x'^2/V_*^2$ and $v_y'^2/V_*^2$ as functions of z/δ on channel centreline. The ratio $v_y'^2/v_x'^2$ was in average about 0.28 at all transverse locations, but next to the sidewall. The data showed a good quantitative agreement with the detailed experiments of Xie (1988) and Tachie (2001) in smooth open channel flows. Further details on the initial flow properties were described in Koch and Chanson (2005).

3 Basic flow patterns

Non-intrusive unsteady free-surface measurements were performed for a range of partial gate closure (Table 1). For large gate openings, the surge propagation was slow and the bore front was followed by a train of well-formed undulations: i.e., an undular surge pattern (Fig. 3(a)). At very-low surge Froude numbers ($1 < \mathrm{Fr} < 1.4$ to 1.5), the free-surface undulations had a smooth appearance and no wave breaking wave observed. However some cross-waves, or sidewall shock waves, were seen developing upstream of the first wave crest and intersecting next to the first crest (Fig. 3(a)). The cross-waves propagated behind the first wave crest, they were reflected on the opposite sidewall and they gave a lozenge pattern to the free-surface. A similar cross-wave patterns was observed in stationary undular hydraulic

Table 1 Experimental flow conditions

Run (1)	Q ($\mathrm{m^3\,s^{-1}}$) (2)	d_0 (*) (m) (3)	Gate opening (h) (m) (4)	Surge type at $x = 5$ m (5)	U ($\mathrm{m\,s^{-1}}$) (6)	d_{conj} (*) m (7)	Fr (8)	Remarks (9)
M9	0.0401	0.079	0.010	Breaking	0.682	0.1563	1.93	
M7	0.0400	0.079	0.020	Breaking	0.541	0.1543	1.77	ADV measurements
M6	0.0406	0.0795	0.030	Breaking	0.549	0.1447	1.77	
M8	0.04015	0.079	0.040	Undular (breaking)	0.456	0.1353	1.67	
M4–M5	0.0403	0.0785	0.065	Undular	0.315	0.1199	1.53	
M1	0.0406	0.079	0.070	Undular	0.286	0.1172	1.49	
M2–M3	0.0403	0.07875	0.075	Undular	0.238	0.1092	1.44	
M11	0.0403	0.0795	0.080	Undular	0.235	0.1032	1.41	ADV measurements.
M10	0.0403	0.0795	0.092	Undular	0.140	0.0957	1.31	

Notes: d_{conj}: Conjugate depth measured immediately behind the surge front; h: gate opening after gate closure; U: surge front celerity measured between $x = 6$ and 5 m; (*) measured at $x = 5$ m.

(a)

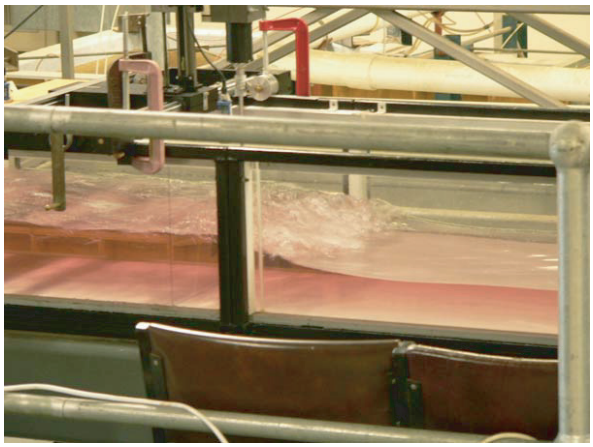

(b)

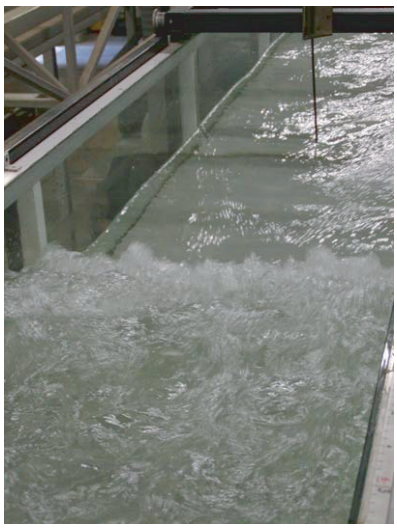

(c)

Figure 3 Photographs of positive surge experiments. (a) Undular surge (Run M11, $Q = 0.040\,\mathrm{m^3\,s^{-1}}$, $d_o = 0.079\,\mathrm{m}$, Fr = 1.4) — Looking downstream at the incoming first wave crest — Note cross-waves developing upstream of the first wave crest and intersecting next to the first wave crest. (b) Undular surge with some breaking at the first crest (Run M8, $Q = 0.040\,\mathrm{m^3\,s^{-1}}$, $d_o = 0.079\,\mathrm{m}$, Fr = 1.67) — The first wave crest is characterised by a small breaking roller — Side view of first wave crest with bore front propagating from left to right. (c) Weak positive surge ($Q = 0.052\,\mathrm{m^3\,s^{-1}}$, $d_o = 0.095\,\mathrm{m}$, $U = 0.82\,\mathrm{m\,s^{-1}}$, Fr = 1.99) — Looking upstream at the bore front propagating upstream (away from camera)

jumps (Chanson and Montes, 1995; Chanson, 1995; Montes and Chanson, 1998; Ohtsu *et al.*, 2001). For some flow conditions, a small "cockscomb" roller was sometimes seen at the first intersection of the cross-waves. For intermediate surge Froude numbers (1.4 to 1.5 < Fr < 1.7), wave breaking was observed at the bore front, and the ensuing free-surface undulations were flatter (Fig. 3(b)). At larger surge Froude numbers (i.e. Fr ≥ 1.7), a breaking surge was seen (Fig. 3(c)). Within the range of present investigations (1.7 ≤ Fr ≤ 2), such a breaking surge was a weak surge. The surge propagated relatively rapidly, and the free-surface appeared to be quasi-two-dimensional. For the entire range of investigations, the bore celerity ranged from 0.14 to $0.7\,\mathrm{m\,s^{-1}}$ (Table 1, column 6), and the flow patterns were overall consistent with earlier studies (e.g. Favre, 1935; Treske, 1994).

Typical instantaneous free-surface profiles are presented in Fig. 4. Each curve shows instantaneous dimensionless flow depth d/d_o as a function of dimensionless time from gate closure $t \times \sqrt{g/d_o}$, where d_o is the initial water depth at $x = 5\,\mathrm{m}$. Figure 4(a) presents an undular surge experiment while Fig. 4(b) illustrates a weak, breaking surge. Note in Fig. 4 a few spurious points and some missing data. The acoustic displacement meter output was a function of the strength of the acoustic signal reflected by the free-surface. When the free-surface was not horizontal, some erroneous points were recorded. These were

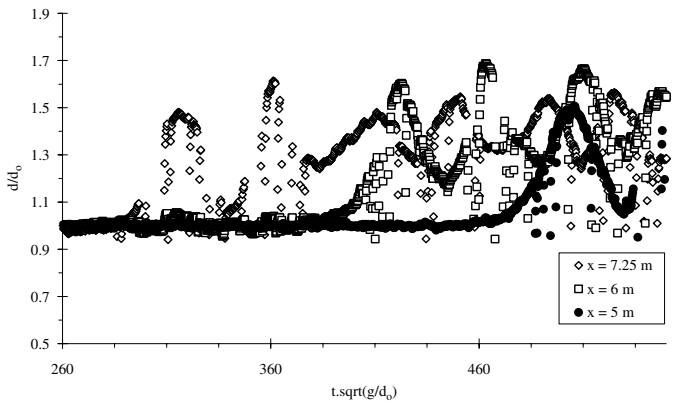

(a)

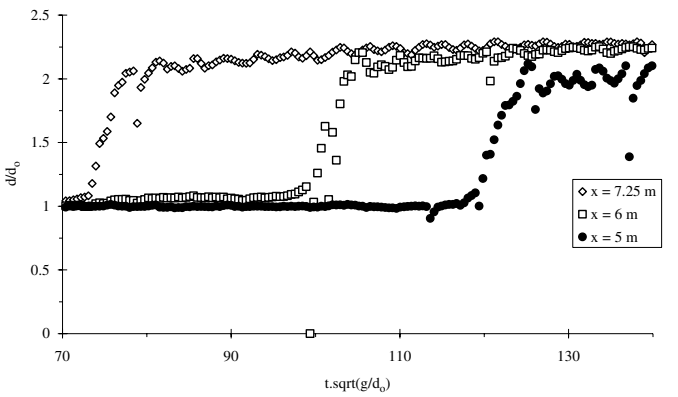

(b)

Figure 4 Instantaneous dimensionless water depth d/d_o at three longitudinal locations ($x = 7.25$, 6 and 5 m, centreline data). (a) Undular surge: $Q = 0.0403\,\mathrm{m^3\,s^{-1}}$, $d_o = 0.0795\,\mathrm{m}$ at $x = 5\,\mathrm{m}$, $h = 0.092\,\mathrm{m}$ (run M10, Fr = 1.3). (b) Weak (breaking) surge: $Q = 0.04003\,\mathrm{m^3\,s^{-1}}$, $d_o = 0.079\,\mathrm{m}$ at $x = 5\,\mathrm{m}$, $h = 0.020\,\mathrm{m}$ (run M7, Fr = 1.8)

relatively isolated and easily ignored. Overall the data showed a gradual evolution of the positive surge shape as it propagated upstream (e.g. from $x = 7$ to 5 m) (Fig. 4). The data suggested a slight reduction in bore height with increasing distance from the downstream gate. The trend was consistent with a fully-developed bore propagating against a gradually-varied flow with the observed S2 backwater profile (e.g. Henderson, 1966).

3.1 Comment

In a fully-developed surge, the ratio of conjugate depths (d_{conj}/d_o) must satisfy the continuity and momentum equations (Eq. (1)). Present experimental results were close to those predicted by the momentum principle, although the data showed slightly lower conjugate depth ratios for $1.1 < Fr < 2$. Several factors may affect the data. In undular surges, the estimate of conjugate depth is somewhat arbitrary. With weak surges, the bore front was associated with some air entrainment in the roller which affected adversely the readouts.

Importantly, a major difference between undular and weak surge is the pressure field and, in turn the velocity field, behind the bore front. In an undular flow, the pressure distributions must deviate from hydrostatic in a manner predicted by ideal-fluid flow theory (e.g. Rouse, 1938, 1959). The free-surface is a streamline and a simple flow net analysis shows that the pressure gradient must be greater than hydrostatic beneath wave trough and less than hydrostatic beneath wave crest. This was observed experimentally in stationary undular jumps (Chanson and Montes, 1995; Montes and Chanson, 1998). The pressure re-distributions between wave crests and troughs induce in turn significant velocity re-distributions between the upstream flow cross section and the first wave crest, and between subsequent crests and troughs.

4 Unsteady velocity measurements in undular surge

In the undular surge, no formed roller was observed and a train of well-formed free-surface undulations followed the first wave crest. Experimental results showed some major effects of undular surge passage on the velocity field. The streamwise velocity V_x decreased sharply with the surge passage and it fluctuated afterwards with the same period as the surface undulations. Maximum velocities were observed beneath wave troughs and minimum velocities below the wave crests at all vertical and transverse locations. In undular flow, irrotational flow theory predicts rapid redistributions of velocity distributions between wave crests and troughs. Present results were generally in agreement with irrotational flow motion although the latter is based upon the assumption of frictionless fluid. It does not account for bed and sidewall friction, nor for the initial flow turbulence.

Large fluctuations of velocities were observed beneath the undulations. The range of velocity fluctuations was larger than that of initial turbulent velocities. For example, in Fig. 5 for $t \times \sqrt{g/d_o} > 90$ to 100. Note that the velocity fluctuation

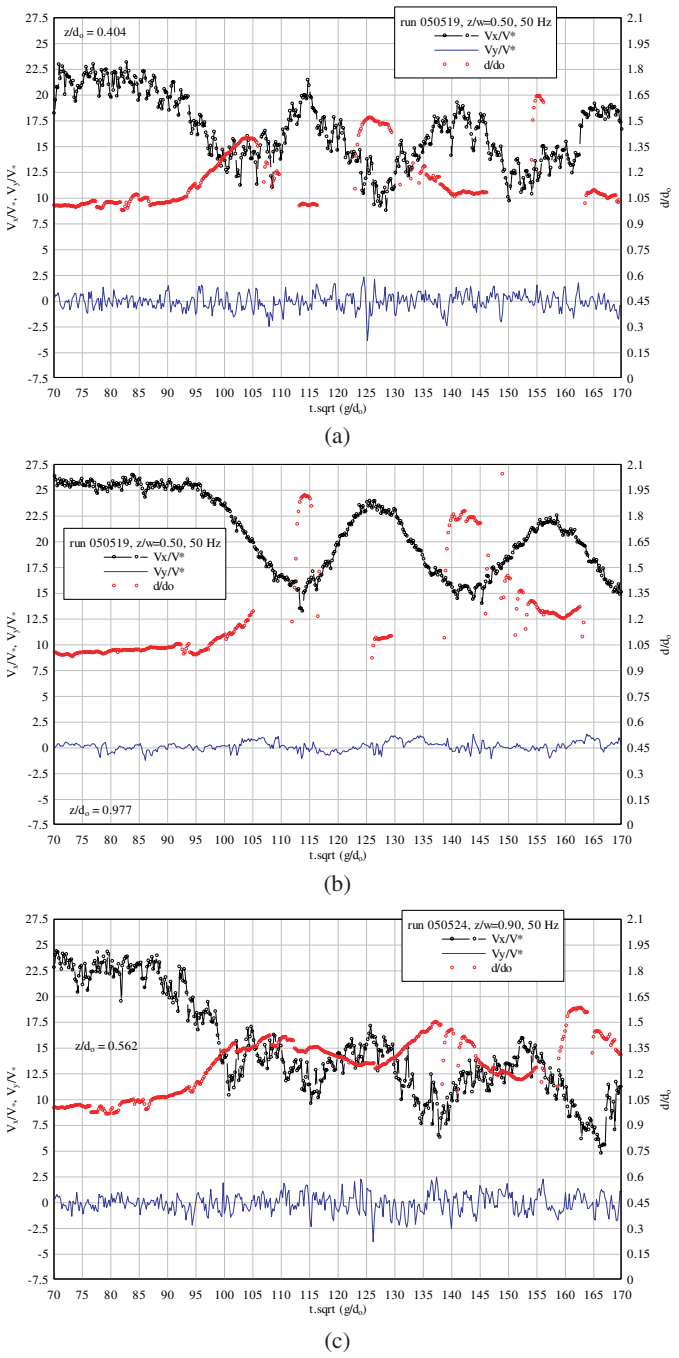

Figure 5 Dimensionless instantaneous depth d/d_o and velocities V_x/V_* and V_y/V_* as functions of dimensionless time $t \times \sqrt{g/d_o}$ beneath an undular surge (Fr = 1.4) at $x = 5.0$ m. (a) Centreline data at $z/d_o = 0.40$, $y/W = 0.5$. (b) Centreline data at $z/d_o = 0.98$, $y/W = 0.5$. (c) Transverse data close to wall at $z/d_o = 0.56$, $y/W = 0.90$

measurements were an Eulerian characterisation of the flow. These included the contributions of both velocity deviations from an ensemble average and time-variation of the ensemble average.

Figure 5 illustrates the effects of an undular surge on the turbulent velocity field at $x = 5.0$ m. It presents instantaneous velocity and free-surface data on the channel centreline, where V^* is the shear velocity on the channel centreline prior to surge arrival ($V^* = 0.044$ m s^{-1}). The time t is zero 10 s prior to the first wave crest passage.

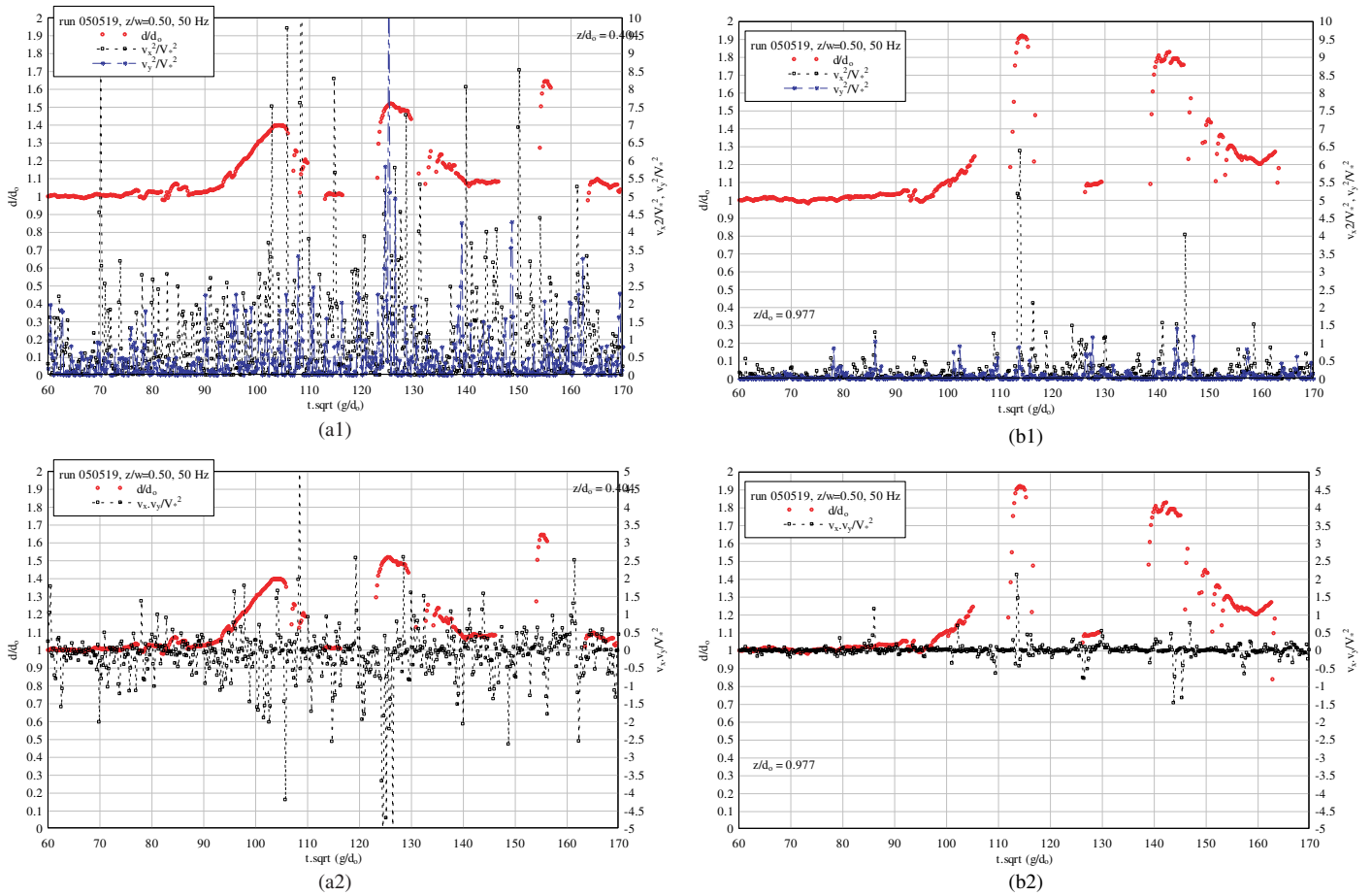

Figure 6 Dimensionless normal and tangential Reynolds stresses (v_x^2/V_*^2, v_y^2/V_*^2, $v_x \times v_y/V_*^2$) beneath an undular surge (Fr = 1.4) on the channel centreline ($y/W = 0.5$). (a) $z/d_o = 0.40$. (a1) Normal Reynolds stresses (v_x^2/V_*^2, $v_y{}^2/V_*^2$) (a2) Tangential Reynolds stress ($v_x \times v_y/V_*^2$). (b) $z/d_o = 0.98$. (b1) Normal Reynolds stresses (v_x^2/V_*^2, v_y^2/V_*^2) (b2) Tangential Reynolds stress ($v_x \times v_y/V^{*2}$)

4.1 Turbulent Reynolds stresses

Reynolds stress data showed large turbulent stresses below the surge front and ensuing undulations (Fig. 6). This is seen in Fig. 6 for $t \times \sqrt{g/d_o} > 90$. Reynolds stress levels were significantly larger than in the initial steady flow. In particular, intense normal stresses, and tangential stresses, were consistently seen beneath wave crests and just before each crest. These turbulent stresses were larger than beneath the adjacent wave troughs (Fig. 6). Further present undular data showed larger Reynolds stresses at the lower sampling locations including next to the bed (e.g. Fig. 6(a)). Comparatively smaller Reynolds stresses were measured at higher sampling locations.

5 Unsteady velocity measurements in weak, breaking surge

5.1 Instantaneous velocity field

Experimental results showed consistently some basic flow feature in weak surges. First the streamwise velocity component decreased rapidly with the passage of the surge front. The sudden increase in water depth yielded a slower flow motion to satisfy the conservation of mass. Second the transverse velocity fluctuations exhibited some marked changes after the surge passage. For example, in Fig. 7(a) and 7(b), for $t \times \sqrt{g/d_o} > 100$. These consisted of relatively larger transverse V_y fluctuation range associated with some low-frequency pattern that may be induced by large vortical structure (i.e., the structure composed of vortices) in the surge roller.

Third, visual observations and recorded data showed that the free-surface elevation rise first slowly immediately prior to the roller (Figs. 7 and 8). This is illustrated in Fig. 8(a) and an explanatory sketch is presented in Fig. 8(b). The "gradual" rise in free-surface was associated with a "gentle" decrease of the mean streamwise velocity component at all vertical elevations. Later the arrival of the roller was marked by a discontinuity of the water depth. In first approximation, the free-surface shape, immediately prior to the roller, was about:

$$\frac{d}{d_o} = 1 + 0.00045 \times \frac{g \times t'^2}{d_o}$$

$$1 < \frac{d}{d_o} \leq 1 + \frac{h_s}{d_o} \qquad (5)$$

where d is the instantaneous water depth, t' is the time at the start of increasing water depth and h_s is the vertical rise in water level immediately prior to the roller toe (Fig. 8(b)). Equation (5) is the best fit of the investigated breaking surge data for Fr = 1.8, and

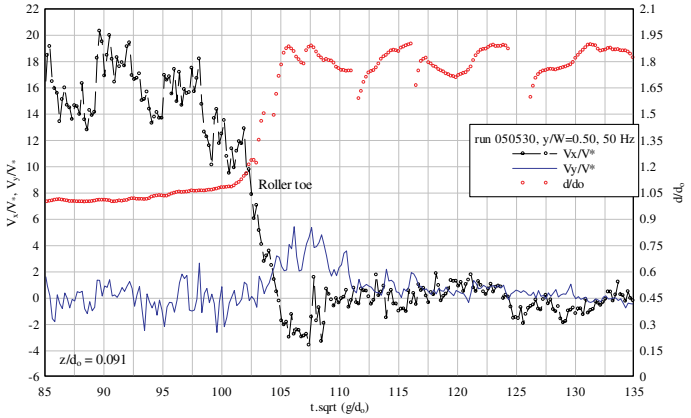

(a)

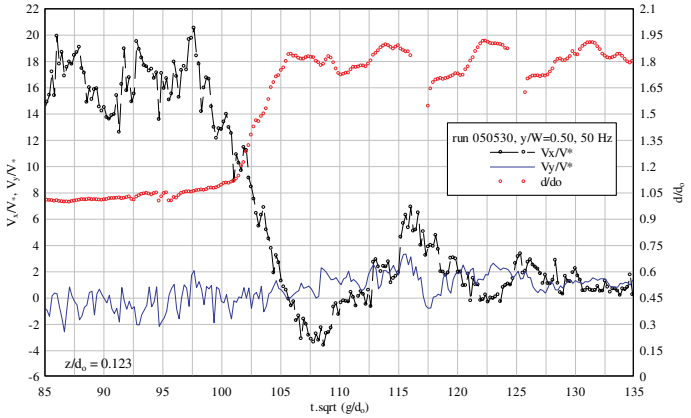

(b)

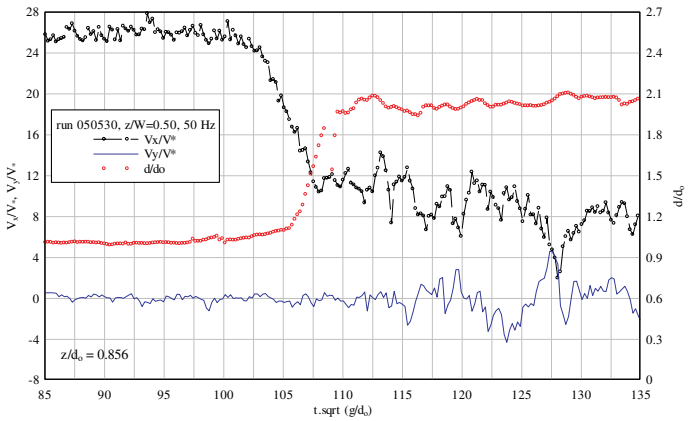

(c)

Figure 7 Dimensionless instantaneous water depth d/d_o and velocity components V_x/V_* and V_y/V^* as functions of dimensionless time $t \times \sqrt{g/d_o}$ beneath the weak surge front (Fr = 1.8, Centreline data, $y/W = 0.5$), (a) $z/d_o = 0.091$. (b) $z/d_o = 0.123$, Series 1 (Fr = 1.8). (c) $z/d_o = 0.86$, Series 1 (Fr = 1.8)

the water elevation h_s was observed to be: $h_s/d_o = 0.1$. Basically the free-surface was seen to curve upwards immediately before the roller toe, in a fashion somehow similar to a spilling breaker situation. However a spilling breaking wave and a positive surge are totally different flow processes. Some data by Hornung *et al.* (1995) showed a similar upward free-surface curve ahead of the roller in positive surge propagating in still water with similar surge Froude number. In stationary hydraulic jumps, some slight free-surface curvature may be seen upstream of the roller but of a lesser magnitude than present weak surge observations.

Fourth, the velocity records showed some marked difference depending upon the vertical elevation z (Figs. 7 and 8(b)). For $z/d_o > 0.5$, the streamwise velocity component decreased rapidly at the surge front although the streamwise velocity V_x data tended to remain positive beneath the roller toe. In contrast, for $z/d_o < 0.5$, the longitudinal velocity became negative although for a short duration on the channel centreline (e.g. Fig. 7(a) and 7(b) for $104 < t \times \sqrt{g/d_o} < 110$). This feature was observed at each transverse location ($0.5 \leq y/W \leq 0.95$). At $y/W = 0.75$, 0.90 and 0.95, the streamwise velocity component would remain negative for some time: e.g., for up to $\Delta t \times \sqrt{g/d_o} \sim 10$ to 30. The existence a sudden longitudinal flow reversal indicated unsteady flow separation beneath the surge front. At a fixed point, it was a relatively rapid transient. The longitudinal flow deceleration yielded negative streamwise V_x velocities with $(V_x/V_*)_{min} \sim -3.5$. This observation was recorded systematically at $z/d_o < 0.2$ on different days and with different sampling rates. The data suggested also increased transverse fluctuations beneath the roller, and the magnitude of maximum transverse velocity fluctuation was substantial: i.e., $(V_y/V_*)_{max} \approx +5$ to 6 in Fig. 7(a) and 7(b).

5.1.1 *Remarks*

Flow separation and recirculation were observed beneath stationary undular hydraulic jumps by Montes (1979), Ohtsu *et al.* (2001) and Chanson (2005). Recirculation was seen typically next to the bed under the first wave crest of undular jumps with partially-developed inflow conditions. But it was acknowledged not to occur in undular jumps with fully-developed inflow conditions (Chanson and Montes, 1995; Ohtsu *et al.*, 2001). Flow separation was never reported beneath a weak hydraulic jumps to date, to the best knowledge of the writers. (Leutheusser and Kartha (1972) indicated that "hydraulic jumps with un-developed inflow tend toward separation with increasing Froude number". But they conducted experiments with $2.85 \leq V_o/\sqrt{g \times d_o} \leq 14.4$, and they did not observe visually nor experimentally flow recirculation!).

5.2 *Turbulent Reynolds stresses in weak surge*

Weak surge data showed large Reynolds stresses beneath the surge front and roller (Fig. 9). This is seen in Fig. 9 for $t \times g/d_o > 100$ to 110. Both normal and tangential stresses were larger than those in the initial steady flow, and this was especially true at $z/d_o > 0.5$. Note in particular the significant magnitude of the transverse normal stresses (Fig. 9(b2)). The findings were consistent with large transverse velocity fluctuations recorded beneath the roller toe and shown in Fig. 7. Very close to the bed, large instantaneous stresses were also observed at the passage of the roller (Fig. 9(a)).

At the highest sampling elevations, large turbulent stresses were observed for relatively long periods: $\Delta t \times g/d_o \sim 120$ to 150 although tangential stresses tended to remain large for longer periods (e.g. Fig. 9(b)). It is believed that the sudden increase in

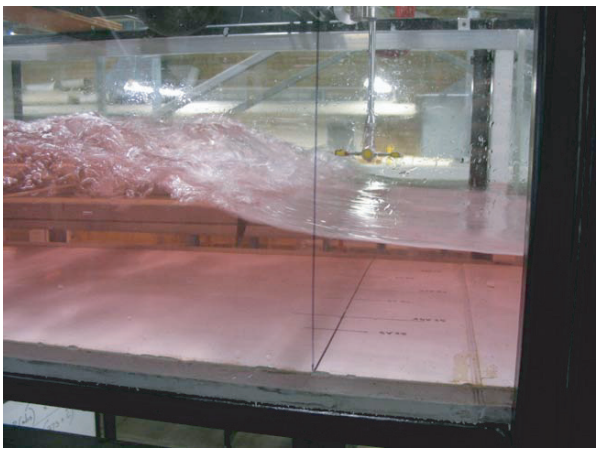

(a)

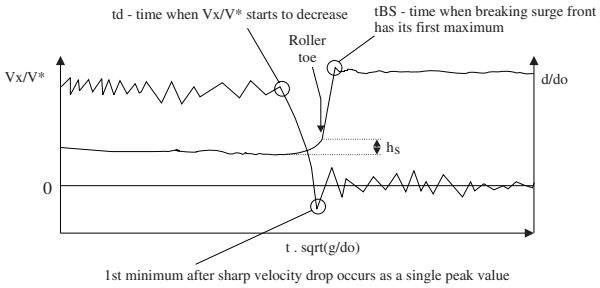

(b1)

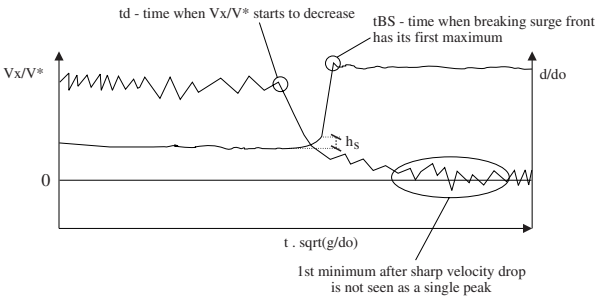

(b2)

Figure 8 Detail of the weak surge front leading edge (Fr = 1.8). (a) Photograph of the advancing front at $x = 5$ m, view through the left sidewall — Bore propagation from left to right. (b) Sketch of instantaneous water depth and streamwise velocity measurements next to the bore front. (b1) Typical record for streamwise velocity component for $z/d_o < 0.5$. (b2) Typical record for streamwise velocity component for $z/d_o > 0.5$

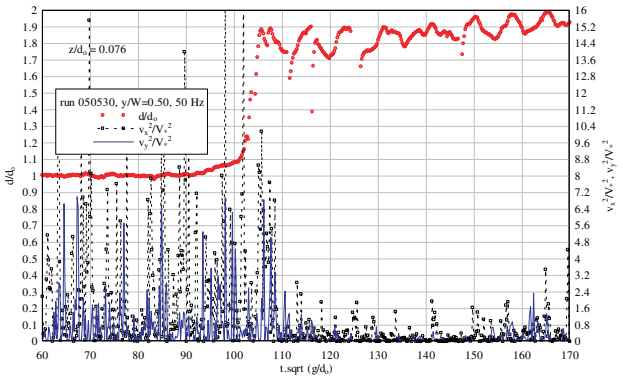

(a1)

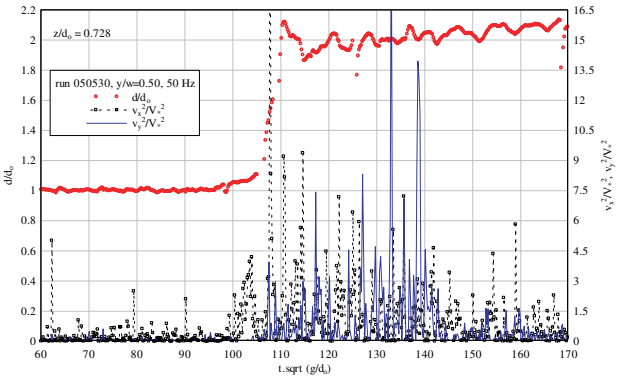

(b1)

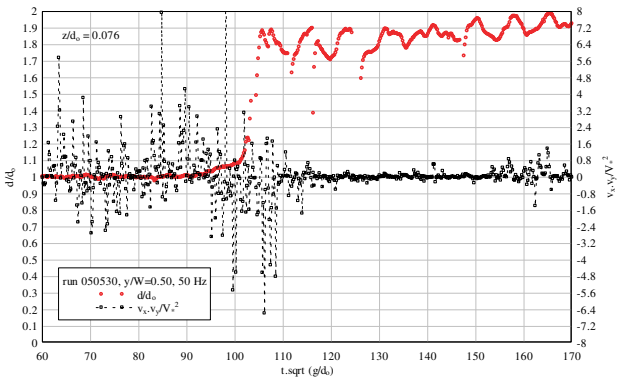

(a2)

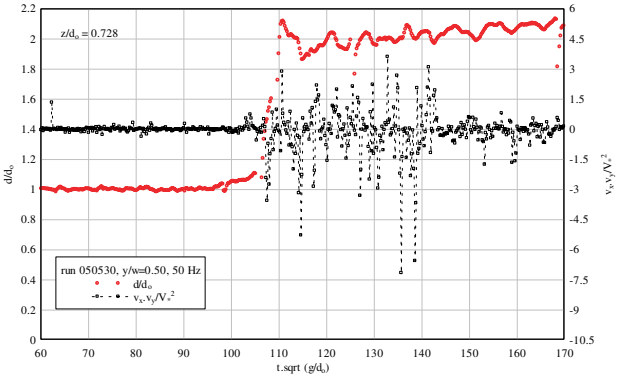

(b2)

Figure 9 Dimensionless normal and tangential Reynolds stresses (v_x^2/V_*^2, v_y^2/V_*^2, $v_x \times v_y/V_*^2$) beneath a weak surge (Fr = 1.8) on channel centreline ($y/W = 0.5$). (a) $z/d_o = 0.076$, Series 1. (a1) Normal Reynolds stresses (v_x^2/V_*^2, $v_y{}^2/V_*^2$). (a2) Tangential Reynolds stress ($v_x * v_y/V_*^2$). (b) $z/d_o = 0.728$, *Series*1. (b1) Normal Reynolds stresses (v_x^2/V_*^2, v_y^2/V_*^2). (b2) Tangential Reynolds stress ($v_x \times v_y/V^{*2}$)

normal and tangential turbulent stresses for $0.5 < z/d_o < 1$ was caused by the developing mixing layer of the roller. (In the present study, no sampling could be conducted for $z/d_o > 1$ and there was no turbulence data in the surge roller itself.)

In stationary hydraulic jumps and related flows, researchers observed similarly large Reynolds stresses in and next to the developing shear layer (Rouse *et al.*, 1959; Resch and Leutheusser, 1972; Liu, 2004).

6 Summary and conclusion

Limited quantitative information is available to date on the turbulence induced by positive surges because the hydrodynamics and turbulence field were not studied with fine instrumentation under well-defined flow conditions. Herein new experimental investigations were conducted under controlled flow conditions in a large channel. Detailed turbulence measurements were performed with a high-temporal resolution (50 Hz) using side-looking acoustic Doppler velocimetry and non-intrusive free-surface measurement devices. The experiments were designed to study a range of positive surges with a minimum number of dependant variables. Using one set of initial flow conditions, experiments were performed in positive surges resulting from a rapid gate closure at the downstream end of the flume and propagating upstream against the initial flow. The only dependant variable was the downstream gate opening after closure.

Two main types of positive surge were observed. For surge Froude numbers Fr less than 1.7, the bore was an undular surge. The wave front was followed by a train of well-formed free-surface undulations. Some breaking was seen at the first wave crest for 1.4 to $1.5 < \text{Fr} < 1.7$. For larger surge Froude numbers ($\text{Fr} > 1.7$), a weak breaking surge was observed. The surge front had a marked roller with some surface upward curvature ahead of the roller, for the range of investigations ($1.7 < \text{Fr} < 2.1$).

Detailed instantaneous velocity measurements showed a marked effect of the surge passage. Streamwise velocities were characterised by a rapid flow deceleration at all vertical elevations, and some flow reversal were measured next to the bed in the weak surge flow. Large fluctuations of longitudinal and transverse velocities were recorded beneath the surges. Turbulent stresses were deduced from high-pass filtered data. The results showed large normal and tangential Reynolds stresses beneath the surge front.

A comparison between undular and weak surge data suggested some basic difference. In weak surge, large stresses were observed next to the shear zone in regions of high velocity gradients, while some unsteady flow recirculation was recorded next to the bed. In undular surges, the largest Reynolds stresses were recorded in the lower flow region including next to the bed, and maximum normal and tangential stresses were observed beneath the wave crests behind the advancing front.

While the present study allowed a detailed comparison between the effects of undular and breaking bores, it was limited to one set of initial flow conditions. Further works should encompass a wider range of inflow conditions and surge generation, including positive propagating downstream.

Acknowledgments

The writers thank Professor Michele MOSSA (Politecnico di Bari, Italy) for his valuable input. They thank also Graham ILLIDGE (The University of Queensland) for his technical assistance. Hubert CHANSON thanks all the people who provided him with relevant information, in particular Dr Minnan LIU for providing her original data.

Notation

d = Flow depth (m) measured normal to the invert
d_{conj} = Conjugate flow depth (m) measured immediately behind the surge front
d_o = Initial flow depth (m) measured normal to the chute invert
Fr = Surge Froude number: $\text{Fr} = (U \pm V)/\sqrt{g^* d}$
g = Gravity constant (m s^{-2}); $g = 9.8 \text{m s}^{-2}$ in Brisbane, Australia
h = Gate opening (m) after gate closure
h_s = Vertical rise (m) in water level in weak surge prior to roller toe
Q = Volume flow rate ($\text{m}^3 \text{s}^{-1}$)
S_o = Bed slope: $S_o = \sin\theta$
t = Time (s)
U = Surge front celerity (m s^{-1}), positive upstream
V = 1-Velocity (m s^{-1}) positive downstream
2-instantaneous velocity (m s^{-1})
V_o = Initial flow velocity (m s^{-1}) positive downstream
V^* = Shear velocity (m s^{-1})
V_x = Streamwise velocity (m s^{-1}) positive downstream
V_y = Transverse velocity (m s^{-1}) positive towards the left sidewall
$\bar{V}$ = Time-averaged velocity (m s^{-1})
v = Turbulent velocity fluctuation (m s^{-1}): $v = V - \bar{V}$
v' = Root mean square of turbulent velocity component (m s^{-1})
v'_x = Root mean square of streamwise component of turbulent velocity (m s^{-1})
v'_y = Root mean square of transverse component of turbulent velocity (m s^{-1})
W = Channel width (m)
x = Longitudinal distance (m) measured from the channel intake, positive downstream
y = Transverse distance (m) measured from the right sidewall
z = Distance (m) normal to the bed; vertical distance (m) for a horizontal channel
Δt = Time period (s)
δ = Boundary layer thickness (m) defined in terms of 99% of the free-stream velocity

Subscript

conj = Conjugate flow conditions: i.e., immediately behind the positive surge front
x = Streamwise component positive downstream
y = Component transverse to the channel (i.e., normal to right sidewall)
o = Initial flow conditions: i.e., upstream of the positive surge front

Abbreviation

CL = Centreline

References

Barré de Saint-Venant, A.J.C. (1871). Théorie et equations générales du mouvement non permanent des eaux courantes. *Comptes Rendus des séances de l'Académie des Sciences*, Paris, France, Séance 17 July 1871, 73, 147–154 (in French).

Benet, F., Cunge, J.A. (1971). Analysis of experiments on secondary undulations caused by surge waves in trapezoidal channels. *J. Hydraul. Res. IAHR* 9(1), 11–33.

Benjamin, T.B., Lighthill, M.J. (1954). On cnoidal waves and bores. *Proc. Royal Soc. of London, Series A, Math. & Phys. Sci.* 224(1159), 448–460.

Boussinesq, J.V. (1877). Essai sur la théorie des eaux courantes. ('Essay on the Theory of Water Flow.') *Mémoires présentés par divers savants à l'Académie des Sciences*, Paris, France, Vol. 23, Série 3, No. 1, supplément 24, 1–680 (in French).

Bradshaw, P. (1971). An introduction to turbulence and its measurement. *Pergamon Press*, Oxford, UK, The Commonwealth and International Library of Science and technology Engineering and Liberal Studies, Thermodynamics and Fluid Mechanics Division, 218.

Chanson, H. (2000). Boundary shear stress measurements in undular flows: Application to standing wave bed forms. *Water Res. Res.* 36(10), 3063–3076.

Chanson, H. (2004a). The hydraulics of open channel flows: An introduction. *Butterworth-Heinemann*, Oxford, UK, 2nd edn, 630.

Chanson, H. (2004b). Environmental hydraulics of open channel flows. *Elsevier Butterworth-Heinemann*, Oxford, UK, 483.

Chanson, H. (2005). Physical modelling of the flow field in an undular tidal bore. *J. Hydraul. Res.*, *IAHR*, 43(3), 234–244.

Chanson, H., Montes, J.S. (1995). Characteristics of undular hydraulic jumps. Experimental apparatus and flow patterns. *J. Hydraul. Engrg., ASCE* 121(2), 129–144. Discussion: 123(2), 161–164.

Chanson, H., Trevethan, M., Aoki, S. (2005). Acoustic doppler velocimetry (adv) in a small estuarine system. field experience and 'despiking'. Jun, B.H., Lee, S.I., Seo, I.W., Choi, G.W. (eds), In: *Proceeding of 31th Biennial IAHR Congress*, Seoul, Korea, Theme E2, Paper 0161, 3954–3966.

Cunge, J.A. (2003). Undular bores and secondary waves — experiments and hybrid finite-volume modelling. *J. Hyd. Res.*, *IAHR* 41(5), 557–558.

Favre, H. (1935). Etude théorique et expérimentale des ondes de translation dans les canaux découverts. ('Theoretical and Experimental Study of Travelling Surges in Open Channels') *Dunod*, Paris, France (in French).

Garcia, C.M., Garcia, M.H. (2006). Characterization of flow turbulence in large-scale bubble-plume experiments. *Experiments in Fluids* 41(1), 91–101.

Goring, D.G., Nikora, V.I. (2002). Despiking acoustic doppler velocimeter data. *J. Hydraul. Engrg., ASCE* 128(1), 117–126. Discussion: 129(6), 484–489.

Henderson, F.M. (1966). Open channel flow. *MacMillan Company*, New York, USA.

Hornung, H.G., Willert, C., Turner, S. (1995). The flow field downsteam of a hydraulic jump. *J. Fluid Mech.* 287, 299–316.

Koch, C., Chanson, H. (2005). An experimental study of tidal bores and positive surges: Hydrodynamics and turbulence of the bore front. *Report No. CH56/05*, Department of Civil Engineering, The University of Queensland, Brisbane, Australia, July, 170.

Lemmin, U., Lhermitte, R. (1999). ADV measurements of turbulence: Can we improve their interpretation? Discussion. *J. Hydrual Engrg., ASCE* 125(6), 987–988.

Lemoine, R. (1948). Sur les ondes positives de translation dans les canaux et sur le ressaut ondulé de faible amplitude. ('On the Positive Surges in Channels and on the Undular Jumps of Low Wave Height') *Jl La Houille Blanche*, Mar–Apr., 183–185 (in French).

Leutheusser, H.J., Kartha, V.C. (1972). Effects of inflow condition on hydraulic jump. *J Hydrual. Div., ASCE* 98(HY8), 1367–1385.

Liggett, J.A. (1994). Fluid mechanics. *McGraw-Hill*, New York, USA.

Liu, M. (2004). Turbulence structure in hydraulic jumps and vertical slot fischways. Ph.D. thesis., Department of Civil and Enviormental Engineering, University of Alberta, Edmonton, Canada, 313.

McLelland, S.J., Nicholas, A.P. (2000). A new method for evaluating errors in high-frequency ADV measurements. *Hydrological Processes* 14, 351–366.

Montes, J.S. (1979). Undular hydraulic jump — discussion. *J. Hydraul. Div., ASCE* 105(HY9), 1208–1211.

Montes, J.S. (1986). A study of the undular jump profile. *Proceeding of 9th Australasian Fluid Mechanics Conference AFMC*, Auckland, New Zealand, 148–151.

Montes, J.S., Chanson, H. (1998). Characteristics of undular hydraulic jumps. Results and calculations. *J. Hydraul. Engrg., ASCE* 124(2), 192–205.

Nikora, V. (2004). *Person. Comm.*, July, Gold Coast, Australia.

Ohtsu, I., Yasuda, Y., Gotoh, H. (2001). Hydraulic condition for undular-jump formations. *J Hydraul. Res., IAHR* 39(2), 203–209. Discussion: (2002). 40(3), 379–384.

Peregrine, D.H. (1966). Calculations of the development of an undular bore. *J. Fluid Mech.* 25, 321–330.

Piquet, J. (1999). Turbulent Flows. Models and Physics. Springer, Berlin, Germany, 761.

Ponsy, J., Carbonnell, M. (1966). Etude Photogrammétrique d'Intumescences dans le Canal de l'Usine d'Oraison (Basses-Alpes). ('Photogrammetric Study of Positive Surges in the Oraison Powerplant Canal') *J. Soc. Française de Photogram* 22, 18–28.

Rayleigh, L. (1908). Note on tidal bores. *Proc. Royal Soc. of London, Series A Containing Papers of a Mathematical and Physical Character* 81(541), 448–449.

Resch, F.J., Leutheusser, H.J. (1972). Reynolds stress measurements in hydraulic jumps. *J Hydraul. Res., IAHR* 10(4), 409–429.

Rouse, H. (1938). Fluid Mechanics for Hydraulic Engineers. *McGraw-Hill Publ.*, New York, USA (also Dover Publ., New York, USA, 1961, 422).

Rouse, H. (1959). Advanced Mechanics of Fluids. John Wiley, New York, USA, 444.

Rouse, H., Siao, T.T., Nagaratnam, S. (1959). Turbulence characteristics of the hydraulic jump. *Transactions, ASCE* 124, 926–950.

Sander, J., Hutter, K. (1991). On the development of the theory of the solitary wave. A historical essay. *Acta Mechanica* 86, 111–152.

Sandover, J.A., Holmes, P. (1962). The hydraulic jump in trapezoidal channels. *Water Power* 14, 445–449.

Serre, F. (1953). Contribution à l'etude des ecoulements permanents et variables dans les canaux. ('Contribution to the Study of Permanent and Non-Permanent Flows in Channels.') *Jl La Houille Blanche*, 830–872 (in French).

Sobey, R.J., Dingemans, M.W. (1992). Rapidly varied flow analysis of undular bore. *J. Waterway, Port, Coastal and Ocean Engrg., ASCE* 118(4), 417–436.

Tachie, M.F. (2001). Open channel turbulent boundary layers and wall jets on rough surfaces. Ph.D. Thesis, Dept. of Mech. Eng., Univers. of Saskatchewan, Canada, 238.

Teles da Silva, A.F., Pererine, D.H. (1990). Nonsteady computations of undular and breaking bores. *Proceeding of the 22nd International Congress Coastal Engineering*, Delft, The Netherlands, ASCE Publ., 1, 1019–1032.

Treske, A. (1994). Undular bores (favre-waves) in open channels — Experimental studies. *J. Hydrual. Res., IAHR* 32(3), 355–370. Discussion: 33(3), 274–278.

Tricker, R.A.R. (1965). Bores, Breakers, Waves and Wakes. American Elsevier Publ. Co., New York, USA.

Voulgaris, G., Trowbridge, J.H. (1998). Evaluation of the acoustic Doppler Velocimeter (ADV) for turbulence measurements. *J. Atmosph. Oceanic Tech.* 15, 272–289.

Wahl, T.L. (2003). Despiking acoustic Doppler Velocimeter data. Discussion. *J. Hydrual. Engrg., ASCE* 129(6), 484–487.

Wilkinson, D.L., Banner, M.L. (1977). Undular bores. *Proceeding of 6th Australasian Hydrualic and Fluid Mechanics Conferance*, Adelaide, Australia, 369–373.

Xie, Q. (1998). Turbulent flows in non-uniform open channels: experimental measurements and numerical modelling. Ph.D. Thesis, Deptartment of Civil Engineering., University of Queensland, Australia, 339.

Yeh, H.H., Mok, K.M. (1990). On turbulence in bores. *Physics of Fluids*, Series A, 2(5), 821–828.

Zienkiewicz, O.C., Sandover, J.A. (1957). The undular surge wave. *Proceeding of the 7th IAHR Congress*, Vol. II, Lisbon, Portugal, paper D25, D1–11.

Audiovisual bibliography

Lespinasse, P. (2005). "Sons of the Moon." Grand Angle production, France, 50 min.

NHK Japan Broadcasting Corp (1989). "Pororoca: the backward flow of the Amazon". *Videocassette VHS colour*,

NHK, Japan, 29 minutes. (Also Films for the Humanities, Princeton NJ, USA, 1989.)